Pramana – J. Phys. (2017) 89:57
DOI 10.1007/s12043-017-1458-0

$\gamma\gamma + l + \not{E}_{\mathrm{T}}$ signal of NMSSM at the LHC

JACKY KUMAR

Department of High Energy Physics, Tata Institute of Fundamental Research, Mumbai 400 005, India
E-mail: singlajacky@gmail.com

Published online 5 October 2017

Abstract. In the next-to-minimal supersymmetric Standard Model (NMSSM), a pure singlet-like light pseudoscalar (A_1) can dominantly decay to diphoton mode. In the chargino–neutralino associated production, followed by decays of heavier neutralinos to the lighter ones along with A_1 leads to a final-state $\gamma\gamma + l + \not{E}_{\mathrm{T}}$. In this talk, the enhancement mechanism of diphoton mode of A_1 and its detection possibility in the final-state ($\gamma\gamma + l + \not{E}_{\mathrm{T}}$) at the LHC run-2 are briefly summarized.

Keywords. Higgs; supersymmetry.

PACS Nos **12.60.Jv; 12.10.Dm; 98.80.Cq; 11.30.Hv**

1. Introduction

The next-to-minimal supersymmetric Standard Model (NMSSM) [1] is known for providing an elegant solution for the μ-problem [2] and naturally accommodating the 125 GeV Higgs boson [3], and for its very rich phenomenology at the LHC. The scale invariant superpotential of Z_3-NMSSM in the presence of the singlet superfield $\hat{S}$ reads as

$$\mathcal{W}_{\mathrm{NMSSM}} = \mathcal{W}_{\mathrm{MSSM}}\Big|_{\mu=0} + \lambda\hat{S}\hat{H}_u\hat{H}_d + \frac{\kappa}{3}\hat{S}^3, \qquad (1)$$

where an effective μ-parameter is generated when the singlet scalar S acquires a non-vanishing vacuum expectation value (vev), $\mu_{\mathrm{eff}} = \lambda\langle S\rangle \equiv \lambda v_s$. In NMSSM, the additional scalar and fermion components of $\hat{S}$ leads to extended Higgs and neutralino sectors. Consequently, there are three CP-even, two CP-odd, two charged Higgs states, and five neutralinos in this model. The physical Higgs states are admixtures of doublets H_u, H_d and singlet S. Similarly, the neutralino states are admixtures of bino, wino, Higgsino and singlino $\tilde{S}$. For an excellent review of NMSSM, see ref. [4].

The mixing effects of Higgs bosons and neutralino states can leave strong imprints on the Higgs, dark matter and in some cases also on the flavour physics phenomenology (see [4] and references therein). For example, it is known for quite sometime that light pseudoscalar can give potential contributions to meson–antimeson mixing via the so-called 'double-penguin' diagrams [5–8]. Recently, we have shown that the singlino–Higgsino mixing can give rise to potential contributions to the same at large $\tan\beta = v_u/v_d$ through 'crossed box' diagrams [9].

Here we shall discuss an example of this in the Higgs phenomenology. In the case of almost zero singlet–doublet mixing, the lighter CP-odd Higgs almost decouples from fermions suppressing the $b\bar{b}$ and $\tau\tau$ modes, which are known to be dominant otherwise [10]. In such a scenario, A_1 mainly decays via its diphoton mode. Being singlet-like, it has extremely suppressed cross-section through the direct production modes such as gluon–gluon fusion (ggF) and $b\bar{b}A_1$. But interestingly, it can be produced through the chargino–neutralino associated production. In NMSSM, although the analytic form of the cross-section remains the same as in MSSM, but still via Higgsino–singlino mixing there can be NMSSM effects on it. For example, if $\tilde{\chi}_j^0$ is singlino-dominated, the cross-section is very much suppressed. The typical production cross-section for Higgsino-dominated $\tilde{\chi}_j^0$ is of the order of 10 fb [11]. We focus on the following topology:

$$pp \to \tilde{\chi}_1^{\pm}\,\tilde{\chi}_j^0 \to (\tilde{\chi}_1^0\ell^{\pm}\nu)\,(\tilde{\chi}_1^0 A_1),$$

$$A_1 \to \gamma\gamma, \quad (j = 2, 3).$$

This gives rise to one lepton (l), two photons ($\gamma\gamma$) and missing energy ($\not{E}_{\mathrm{T}}$) in the final state (figure 1). After briefly discussing about the enhancement mechanism for the diphoton mode of A_1, we shall present the results of the simulations. It is found that signal sensitivity is quite encouraging for this final state at LHC run 2.

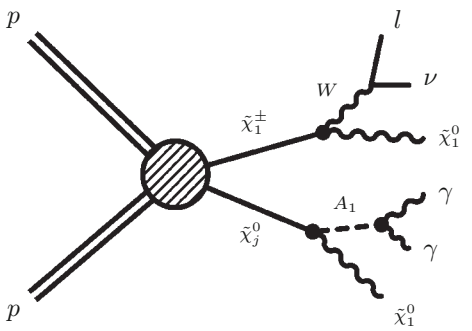

Figure 1. Diagrams for chargino ($\tilde{\chi}_1^{\pm}$)–neutralino ($\tilde{\chi}_j^0$), $j = 2, 3$ associated production in proton–proton collision followed by cascade decays to two photons and a lepton along with the lightest neutralinos.

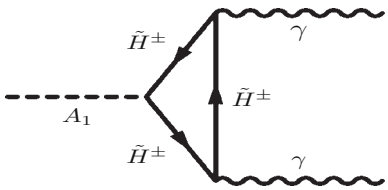

Figure 2. Higgsino contribution to $A_1\gamma\gamma$ coupling.

2. Enhancement of diphoton mode of A_1

To have an enhanced branching ratio in the diphoton mode, A_1 should be purely singlet-like. This leads to the suppression of tree-level fermionic modes such as $b\bar{b}$ and $\tau\tau$. The diphoton mode of singlet-like A_1 is mainly mediated by the Higgsinos (see figure 2). This is an artifact of $\lambda\hat{H}_u\hat{H}_d\hat{S}$ term in the NMSSM superpotential in eq. (1).

To understand the pure singlet limit of A_1, it is instructing to look at CP-odd mass matrix. The initial 3×3 mass matrix in the basis (H_d, H_u, S) reduces to a 2×2 matrix after rotating away the Goldstone mode. In the basis (A, S) it is given by

$$M_P^2 = \begin{pmatrix} M_A^2 & \lambda(A_\lambda - 2\kappa v_s)v \\ \lambda(A_\lambda - 2\kappa v_s)v & M_S^2 \end{pmatrix}, \tag{2}$$

where

$$M_A^2 = \frac{2\mu_{\text{eff}}(A_\lambda + \kappa v_s)}{\sin 2\beta},$$
$$M_S^2 = \lambda(A_\lambda + 4\kappa v_s)\frac{v_u v_d}{v_s} - 3\kappa A_k v_s. \tag{3}$$

The matrix M_P^2 can be diagonalized by performing an orthogonal rotation by an angle α defined by

$$\tan 2\alpha = \frac{2M_{12}^2}{(M_A^2 - M_S^2)}, \tag{4}$$

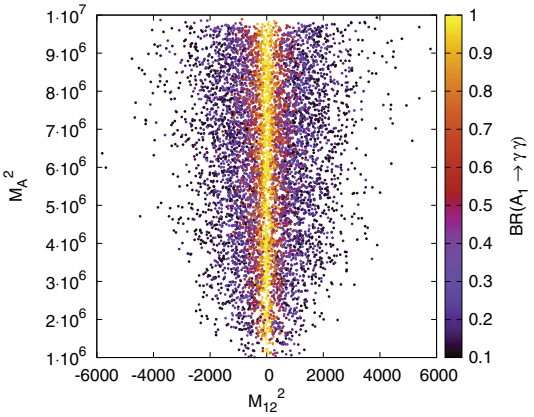

Figure 3. BR($A_1 \to \gamma\gamma$) in the M_A^2–M_{12}^2 plane. All energy units are in GeV.

where $M_{12}^2 = \lambda(A_\lambda - 2\kappa v_s)v$ and $v = 174$ GeV. The mass eigenstates (A_1, A_2) are the mixtures of doublet (A) and singlet (S) weak eigenstates. For the case of singlet-dominated A_1 state, $\sin\alpha$ is very small resulting in the suppression of its couplings with the SM fermions. This is basically a combined effect of the following two conditions:

1. $M_A^2 \gg M_S^2, M_{12}^2$, i.e., the heavier state is too heavy and purely doublet-like whereas the lighter state is singlet-dominated, i.e., a hierarchical mass matrix.
2. $A_\lambda - 2\kappa s \sim 0$, i.e., possible cancellations in the off-diagonal term.

For our numerical study, we scan the NMSSM parameters for the following ranges:

$$\begin{aligned} &0.1 < \lambda < 0.7; \quad 0.1 < \kappa < 0.7; \quad 0 < A_\lambda < 2 \text{ TeV}; \\ &2 < \tan\beta < 50; \quad 140 \text{ GeV} < \mu_{\text{eff}} < 600 \text{ GeV}; \\ &-9 < A_\kappa < -4 \text{ GeV}; \\ &M_{Q_3} = M_{U_3} = 1{-}3 \text{ TeV}; \quad A_t = -3{-}(+3) \text{ TeV}. \end{aligned} \tag{5}$$

The other soft masses are set as

$$\begin{aligned} &M_{Q_{1/2}} = M_{U_{1/2}} = M_{D_{1/2}} = M_{D_3} = 1 \text{ TeV}, \\ &A_b = 2 \text{ TeV}. \end{aligned} \tag{6}$$

The above-mentioned two conditions are illustrated in figure 3, which shows that a hierarchy between M_A^2 and M_{12}^2 is required to arrange large BR (>10%) in the diphoton mode. Also around $M_{12}^2 \sim 0$, the branching ratio can be even more than 90%. Figure 4 shows the corresponding range of $\sin\alpha$ as a function of mass of A_1. The typical values of $\sin\alpha$ for BR($A_1 \to \gamma\gamma$) > 10% are 10^{-4}–10^{-3}.

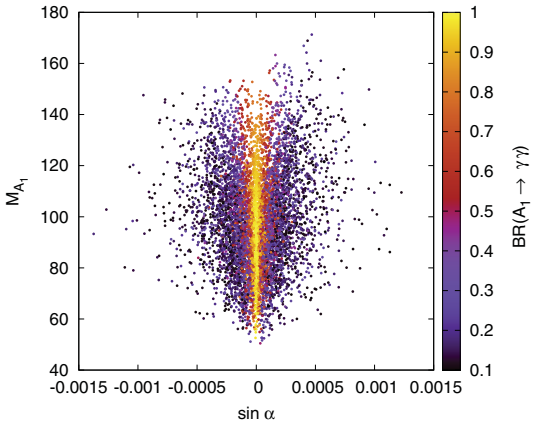

Figure 4. BR($A_1 \to \gamma\gamma$) in the $\sin\alpha$–M_{A_1} plane. All energy units are in GeV.

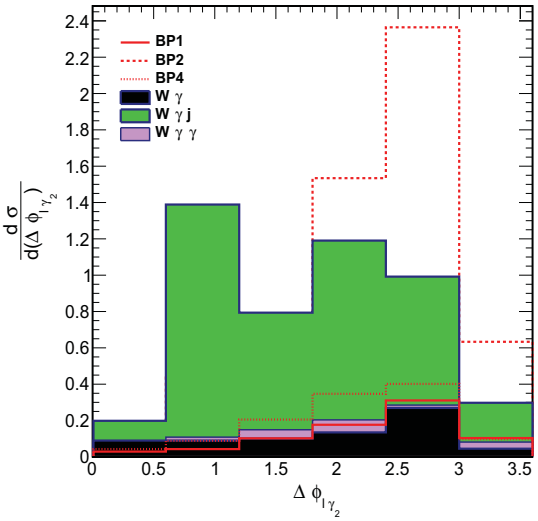

Figure 5. $\Delta\phi_{l\gamma_2}$ distribution for both the signal and the dominant backgrounds.

3. Signal sensitivity

In this section, the results of simulations are summarized. As mentioned before, the signal gets contributions from $\tilde{\chi}_2^0\tilde{\chi}_1^\pm$ as well as $\tilde{\chi}_3^0\tilde{\chi}_1^\pm$ production processes. The dominant SM backgrounds originate from $W\gamma$, $Z\gamma$, $W\gamma\gamma$, $Z\gamma\gamma$ and $Wj\gamma$, $Zj\gamma$, where the second photon can come from the radiation. Using the public library `NMSSMTools` [12], first we obtain the spectra and BRs for benchmark points (BP) shown in table 1 and then generate the signal processes using `PYTHIA6` [13] and obtain the STDHEP files, which are then passed through `Delphes` [14] to take into account the detector effects. Note that the background processes with 3-body final states are generated using `MadGraph` [15].

For signal selection, in an event we demand the two isolated photons satisfying $p_T^{\gamma_1,\gamma_2} \geq 40\,\text{GeV}, 20\,\text{GeV}$, $|\eta^{\gamma_1,\gamma_2}| < 2.4$, and one isolated lepton satisfying $p_T^l \geq 20\,\text{GeV}$, $|\eta^l| < 2.5$ along with missing energy $\not{E}_T \geq 50\,\text{GeV}$. To optimize the signal sensitivity we use an additional selection criterion as

1. $\Delta R_{\gamma_1\gamma_2} = \sqrt{(\eta_{\gamma_1} - \eta_{\gamma_2})^2 + (\phi_{\gamma_1} - \phi_{\gamma_2})^2} \leq 2.0.$

Table 1. Parameters, masses and BRs for six benchmark points (BP).

	BP1	BP2	BP3	BP4	BP5	BP6
λ	0.29	0.40	0.10	0.53	0.64	0.50
κ	0.37	0.45	0.20	0.39	0.36	0.48
$\tan\beta$	6.46	6.46	11.0	4.0	2.5	2.84
M_A	1722	340.7	1311.5	1262.4	1436.9	1655.8
A_κ	−4.97	−4.97	−3.9	−5.8	−6.5	−9.37
μ_{eff}	342.4	200.0	158.5	365.4	636.8	540.7
M_1	300	150.0	135.4	275.9	605.8	514.0
M_2	606.6	606.6	1000.0	9000	1857.4	1597.1
$M_{\tilde{\chi}_1^0}$	280.6	131.4	113.4	261.8	578.3	488.5
$M_{\tilde{\chi}_2^0}$	356.4	210.0	169.0	379.1	657.5	559.8
$M_{\tilde{\chi}_3^0}$	356.7	215.6	182.3	385.5	661.0	572.7
$M_{\tilde{\chi}_1^+}$	340.0	199.3	161.7	377.5	648.6	550.6
M_{A_1}	62	76	63.1	105.2	62.8	66.8
M_{H_1}	124	124	124	124	125	123
BR($\chi_2^0 \to \tilde{\chi}_1^0 A_1$)	0.92	0.83	0.0	0.44	0.98	0.05
BR($\chi_3^0 \to \tilde{\chi}_1^0 A_1$)	0.27	0.31	0.52	0.002	0.11	0.97
BR($A_1 \to \gamma\gamma$)	0.79	0.91	0.98	0.87	0.97	0.97
$\Gamma(A_1 \to \gamma\gamma)$	2.8E-9	2.5E-8	1.3E-9	3.6E-8	3.4E-9	3.5E-9

Table 2. Event summary for the signal and backgrounds (Bkg) subject to a set of cuts. The last column presents the cross-section after multiplying the acceptance efficiency including BRs.

	Process	σ (NLO)	N_{ev}	$N_\gamma \geq 2$	$N_l = 1$	$\not{E}_T \geq 50$	$\Delta R_{\gamma_1\gamma_2} \leq 2$	$\Delta\phi_{l\gamma_2} \geq 1.5$	$\sigma \times \epsilon$ (fb)
BP1	$\tilde{\chi}_2^0\tilde{\chi}_1^\pm$	36.4 fb	0.3L	7124	886	569	502	426	0.38
	$\tilde{\chi}_3^0\tilde{\chi}_1^\pm$	44.8 fb	0.3L	7006	879	587	519	431	0.14
BP2	$\tilde{\chi}_2^0\tilde{\chi}_1^\pm$	335 fb	0.3L	9303	1140	590	415	346	2.9
	$\tilde{\chi}_3^0\tilde{\chi}_1^\pm$	442 fb	0.3L	9593	1213	682	499	418	1.7
BP3	$\tilde{\chi}_3^0\tilde{\chi}_1^\pm$	539 fb	0.3L	5755	589	312	270	240	2.2
BP4	$\tilde{\chi}_2^0\tilde{\chi}_1^\pm$	61.1 fb	0.3L	14750	2555	1916	910	738	0.6
	$\tilde{\chi}_3^0\tilde{\chi}_1^\pm$	43.9 fb	0.3L	14827	2447	1873	935	730	0.002
BP5	$\tilde{\chi}_2^0\tilde{\chi}_1^\pm$	4.00 fb	0.3L	7798	1023	715	598	475	0.060
	$\tilde{\chi}_3^0\tilde{\chi}_1^\pm$	1.80 fb	0.3L	8292	1111	809	694	540	0.003
BP6	$\tilde{\chi}_2^0\tilde{\chi}_1^\pm$	8.80 fb	0.3L	7549	893	497	353	288	0.004
	$\tilde{\chi}_3^0\tilde{\chi}_1^\pm$	4.90 fb	0.3L	9135	1132	813	634	517	0.080
Bkg	$W\gamma$	215 pb	30M	15002	1117	272	65	47	0.33
	$Z\gamma$	103 pb	30M	14792	1506	52	12	10	0.03
	$W\gamma j$	125 pb	2.1M	2987	282	137	49	30	1.80
	$Z\gamma j$	45 pb	2.1M	2531	1203	27	10	6	0.13
	$W\gamma\gamma$	407 fb	0.5L	6011	760	260	66	47	0.40
	$Z\gamma\gamma$	257 fb	0.5L	5312	233	12	7	4	0.02

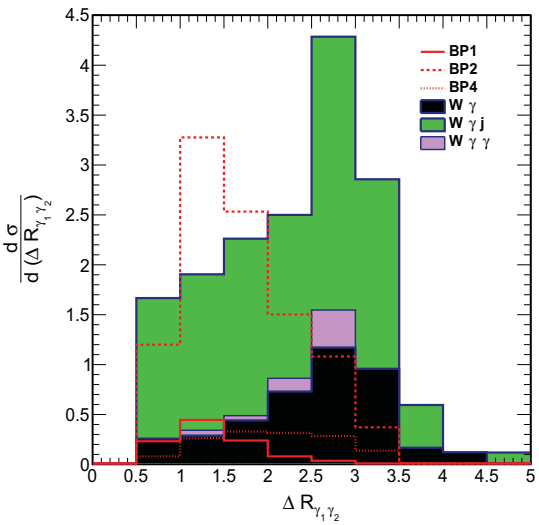

Figure 6. $\Delta R_{\gamma_1\gamma_2}$ distributions for both the signal and the dominant backgrounds.

2. $\Delta\phi_{\ell\gamma_2} > 1.5$, $\Delta\phi_{\ell\gamma_2}$ is the difference in the azimuthal angle between the lepton and the sub-leading photon.

In figures 6 and 5, we display the distributions of $\Delta R_{\gamma_1\gamma_2}$ and $\Delta\phi_{\ell\gamma_2}$ for BP1, BP2 and BP4 as defined in table 1 along with dominant backgrounds. We observe a clear distinction between the signal and the background processes. Table 2 presents the event summary after the various cuts discussed above. The last column shows the cross-section multiplied by the efficiencies after various selections. In table 3, the significance $S/\sqrt{B}$ is estimated for three integrated luminosity options. For

Table 3. The signal cross-sections after multiplying the acceptance efficiency including BRs (2nd row) and significance ($S/\sqrt{B}$) for three integrated luminosity options 100, 300 and 1000 fb^{-1}. The total background cross-section is 2.74 fb.

Process	BP1	BP2	BP3	BP4	BP5	BP6
$\sigma \times \epsilon$ (fb)	0.52	4.6	2.2	0.6	0.063	0.084
$\mathcal{L}$ (fb^{-1})	$S/\sqrt{B}$					
100	3.1	28.1	13.3	3.5	0.40	0.50
300	5.4	48.7	23.9	6.0	0.67	0.88
1000	9.8	89.0	42.0	11.0	1.22	1.60

the benchmark points BP1–BP4 it can be more than 5σ for the 100 fb^{-1} luminosity option. For BP5 and BP6, it degrades severely due to the suppressed production cross-sections due to heavier neutralino masses. It is also found that a much better significance can be obtained if we select the events around for invariant mass of two photons in the range $M_{A_1} \pm 3$ GeV.

4. Conclusions

In NMSSM, the singlet-dominated pseudoscalar can have very much suppressed couplings with the down-type quarks, resulting in the suppression of $b\bar{b}$ and $\tau\tau$ decay modes. Due to this, the diphoton mode is enhanced. We employ this feature and propose a novel signature for the pseudoscalar Higgs boson producing it via chargino-neutralino associated production. This leads to final-state $\gamma\gamma + l + \not{E}_T$. Performing detector

level simulation, the signal sensitivity is estimated for LHC run 2 experiments. We found that this signal is quite robust even for an integrated luminosity of 100 fb^{-1}.

Acknowledgements

The author is grateful to the organizers for an invitation to the conference. He is also thankful to Monoranjan Guchait for collaboration in this work.

References

[1] P Fayet, *Nucl. Phys. B* **90**, 104 (1975), doi:10.1016/0550-3213(75)90636-7
[2] J E Kim and H P Nilles, *Phys. Lett. B* **138**, 150 (1984), doi:10.1016/0370-2693(84)91890-2
[3] L J Hall, D Pinner and J T Ruderman, *J. High Energy Phys.* **1204**, 131 (2012), doi:10.1007/JHEP04(2012)131, arXiv:1112.2703 [hep-ph]
[4] U Ellwanger, C Hugonie and A M Teixeira, *Phys. Rep.* **496**, 1 (2010), doi:10.1016/j.physrep.2010.07.001, arXiv:0910.1785 [hep-ph]
[5] A Crivellin and Y Yamada, *J. High Energy Phys.* **1511**, 056 (2015), arXiv:1508.02855 [hep-ph]
[6] R N Hodgkinson and A Pilaftsis, *Phys. Rev. D* **78**, 075004 (2008), doi:10.1103/PhysRevD.78.075004, arXiv:0807.4167 [hep-ph]
[7] G Hiller, *Phys. Rev. D* **70**, 034018 (2004), arXiv:hep-ph/0404220
[8] F Domingo and U Ellwanger, *J. High Energy Phys.* **0712**, 090 (2007), doi:10.1088/1126-6708/2007/12/090, arXiv:0710.3714 [hep-ph]
[9] J Kumar and M Paraskevas, *J. High Energy Phys.* **1610**, 134 (2016), arXiv:1608.08794 [hep-ph]
[10] M Guchait and J Kumar, *Int. J. Mod. Phys. A* **31(2)**, 1650069 (2016), doi:10.1142/S0217751X1650069X, arXiv:1509.02452 [hep-ph]
[11] M Guchait and J Kumar, *Phys Rev. D* **95(3)**, 035036 (2017), doi:10.1103/PhysRevD.95.035036, arXiv:1608.05693 [hep-ph]
[12] U Ellwanger, J F Gunion and C Hugonie, *J. High Energy Phys.* **0502**, 066 (2005), doi:10.1088/1126-6708/2005/02/066, arXiv:hep-ph/0406215
[13] T Sjostrand, S Mrenna and P Z Skands, *J. High Energy Phys.* **0605**, 026 (2006), doi:10.1088/1126-6708/2006/05/026, arXiv:hep-ph/0603175
[14] DELPHES 3 Collaboration: J de Favereau *et al*, *J. High Energy Phys.* **1402**, 057 (2014), doi:10.1007/JHEP02(2014)057, arXiv:1307.6346 [hep-ex]
[15] J Alwall *et al*, *J. High Energy Phys.* **1407**, 079 (2014), doi:10.1007/JHEP07(2014)079, arXiv:1405.0301 [hep-ph]